

Competition of Diffusion and Crosslink on the Interphase Region in Carbon Fiber/Epoxy Analyzed by Multiscale Simulations

Min Li,¹ Yi-Zhuo Gu,¹ Yan-Xia Li,¹ Hong Liu,² Zuo-Guang Zhang¹

¹Key Laboratory of Aerospace Materials and Performance (Ministry of Education), School of Materials Science and Engineering, Beihang University, Beijing 100191, China

²Institute of Theoretical Chemistry, State Key Laboratory of Theoretical and Computational Chemistry, Jilin University, Changchun 130023, China

Correspondence to: M. Li (E-mail: leemy@buaa.edu.cn)

ABSTRACT: Molecular diffusion and crosslink between sizing, epoxy, and hardener agent were simulated to elucidate forming process of interphase in carbon fiber/epoxy composite, by using a multiscale method, in which fully atomistic molecular dynamics (MD), coarse-grained dissipative particle dynamics (DPD) and Monte Carlo-like polymerizing models are used in combination. It shows that mutual diffusions of the three components tend to result in gradient distributions in the fiber vicinity crossing the interphase transition region. The diffusion behavior is extremely restrained by the crosslink reactions. The results indicate that a period of diffusion before the initiation of chemical reaction is necessarily important to obtain sufficient crosslink within the interphase. The sizing amount and the sizing compositions have significant influence on the interphase region. Thicker sizing layer leads to less crosslink and wider transition region, whereas existence of hardener agent in the sizing layer can generate higher crosslink density without changing the width of the interphase. These results deepen our understanding on molecular formation and optimization of the three-dimensional interphase region in carbon fiber/epoxy composites. © 2013 Wiley Periodicals, Inc. *J. Appl. Polym. Sci.* **2014**, *131*, 40032.

KEYWORDS: composites; crosslinking; surfaces and interfaces; synthesis and processing; theory and modeling

Received 3 July 2013; accepted 3 October 2013

DOI: 10.1002/app.40032

INTRODUCTION

The interphase of fiber composite is deemed as a three-dimensional region, which has different chemical, physical, and mechanical properties from the bulk fiber and matrix material. It has been well demonstrated that the interphase has significant influence on the composite properties.^{1–3} Numbers of micromechanical studies have been conducted to elucidate the interphase role.^{1–7} Commercial carbon fibers (CF) are always coated by a layer of sizing agent to enhance the handleability, which will inevitably impact wetting, reaction, and interfacial properties between the carbon fiber and resin.^{8–12} However, scant information is available on the interphase region at molecular level, which is crucial for optimizing the interphase to produce advantageous interactions between carbon fiber and epoxy matrix and to maximize potential performance of the two main constituents.

Computer simulation, as a feasible route for validating experimental results and predicting new phenomena, becomes especially important on presenting microscopic network structures and the corresponding physical properties.¹³ Coarse-grained (CG) simulation models for polymer networks were firstly developed since 1990s, and the results improved the under-

standing on polymer network formation and properties.^{14–20} To reflect the local network structures of specific polymer systems with atomistic details, atomistic molecular dynamics (MD) simulation method was mostly chosen.^{21–23}

Here, the diffusion and crosslink behavior are investigated to elucidate the interphase formation in-between carbon fiber and epoxy for the composite, by using an innovative multiscale simulation method. The comprehensive details of the simulation method are described elsewhere.^{19,24} This article aims to analyze competition and interplay between the diffusion and the crosslink curing process. Influencing factors, including the processing temperature scheme, the sizing layer thickness, and existence of hardener in the sizing layer are investigated. The results will deepen our understanding on molecular formation and tune mechanism of the three-dimensional interphase region in carbon fiber/epoxy composites.

EXPERIMENTAL

The simulation methodology is briefly introduced here; further details are described in Refs. 19 and 24. In our simulation the input parameters and the boundary conditions were mostly

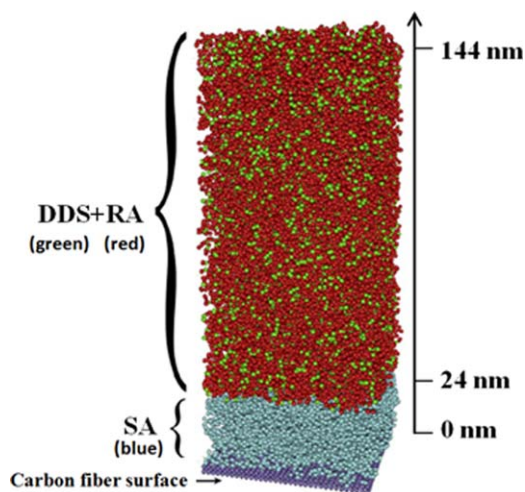


Figure 1. Schematic illustration of the simulation model based on carbon fiber surface, in which widths of the sizing layer and the resin phase are denoted along the vertical axis at the right side. [Color figure can be viewed in the online issue, which is available at wileyonlinelibrary.com.]

assigned according to experimental data. The simulation model system is schematically illustrated in Figure 1, in which 0–24 nm is the sizing layer and 24–144 nm is the resin phase. The bottom is the intrinsic carbon fiber surface which was chemically inert and impenetrable. The resin phase was composed of diglycidyl ether of bisphenol A (denoted as RA) and diamino diphenyl sulfone (denoted as DDS), with the molar ratio of 2 : 1 between RA and DDS. The sizing agent (denoted as SA) was proved to be epoxy-type.⁸ For simulation simplicity the chemical structure of SA was treated the same to that of RA. Note that there was no hardener in the sizing layer.

Based on the molecular mass and the active groups of RA, DDS, and SA, the CG schemes were treated as: one bead representing DDS, two beads representing RA, and ten beads representing SA long chains.²⁵ All diffusion and crosslink simulations were started from the configuration in Figure 1. Newton's equations and Lowe–Andersen (LA) thermostat was employed to describe motions and interactions between the CG beads.^{26–29} Values of dissipative particle dynamics (DPD) parameters were estimated from the Flory–Huggins parameters and the solubility parameters.^{30,31}

Monte Carlo-like probability P_r was employed to control the crosslink kinetics for the simulations.²⁰ For the first step reaction between primary amine and epoxide, $P_r = 0.001$ was defined; for the second step reaction $P_r = 0.0001$; and the third step reaction was neglected in the simulations.^{19,24,32} The

simulation time unit was evaluated to be 361 ms of the real time, by fitting the conversion profile of epoxide in the resin system measured by *in situ* FTIR. Note that, the DPD simulation obeys the same evolution clock to the crosslink simulation.

The molecular distribution of each component and functional group were predicted via relative content (i.e., volume fraction of the concerned CG bead) by running the multiscale simulations. Unless otherwise specified, according to standard manufacturing conditions of the CF/RA composite, a two-stage simulation scheme is always performed to analyze competition between the diffusion and the crosslink behavior. At the first stage, mutual diffusions between components are solely simulated, in which RA and DDS diffuse from the resin phase into the sizing layer, and in contrast SA diffuses oppositely. At the second stage, diffusion and crosslink are simultaneously switched on based on the final state of the first stage. Then distributions of the generated chemical groups, such as the crosslink points, hydroxyl, reacted amines, and unreacted epoxide are presented. To analyze the temperature effect on the interdiffusion behavior of the components, three different diffusion temperatures were set according to the recommended curing cycle for the CF/RA composite system, namely, a standard diffusion temperature at 150°C, a relatively lower one at 110°C, and a relatively higher one at 180°C. Differential scanning calorimetric analysis showed that for RA and DDS system, at 110°C the chemical reaction is fairly slow and can be negligible, while at 180°C the chemical reaction is appropriate and it is recommended as a standard for the resin curing. Hence, we can infer that, actually, at temperature of 110°C the component interdiffusion may solely take place but at 180°C the interdiffusion will happen with progressive chemical reactions simultaneously.

To analyze effect of the sizing layer on the interphase formation, three simulation systems are investigated in this article, denoted as T3-Siz-RA, T3-Sizcur-RA, and C3-Siz-RA, respectively. Note that, unless otherwise specified, the simulation schemes are all performed with T3-Siz-RA, as illustrated in Figure 1. In the T3-Sizcur-RA system, a certain amount of hardener agent originally exists in the sizing layer, however, in T3-Siz-RA and C3-Siz-RA, no hardener is contained in the sizing layer. The sizing amount in C3-Siz-RA is relatively larger, with the thickness of 36 nm, while the sizing layer is 24 nm in the other two systems. Table I lists details of the three simulation systems.

RESULTS AND DISCUSSION

Competition of Diffusion and Crosslink

First, the distribution evolution of each component was analyzed due to diffusions. In Figure 2, at moment of 0.5 min all

Table I. The Construction Parameters and Compositions of Three Simulation Systems, in which Molar Ratio between the Components in One Phase is Described in the Following Brackets

	Thickness of the sizing phase (nm)	Compositions of the sizing phase	Thickness of the resin phase (nm)	Compositions of the resin phase
T3-Siz-RA	24	SA	120	RA+DDS (2 : 1)
T3-Sizcur-RA	24	SA+DDS (4 : 1)	120	RA+DDS (2 : 1)
C3-Siz-RA	36	SA	108	RA+DDS (2 : 1)

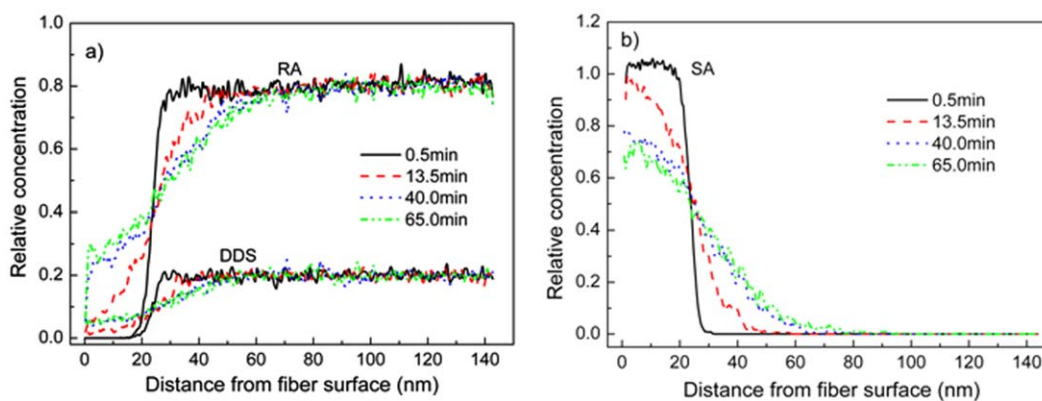


Figure 2. The distribution evolutions of: (a) DDS and RA; and (b) SA, during the diffusion process at 180°C. [Color figure can be viewed in the online issue, which is available at wileyonlinelibrary.com.]

the components stay mainly in the original scope (i.e., RA and DDS in 24–144 nm and SA in 0–24 nm). After 13.5 min, the RA and DDS molecules diffuse onto the carbon fiber surface (i.e., 0 nm), and SA diffuse into the resin phase to 50 nm position. Subsequently, more and more RA and DDS molecules diffuse onto the fiber surface, leading to increase of the concentrations. From 40.0 to 65.0 min, the distributions show only slight evolutions for RA, DDS, and SA. Hence, we can infer that the mutual diffusions are approaching steady equilibrium state after 65.0 min at 180°C. The forefronts of DDS and RA molecules indicate that the two components have approximately equivalent diffuse activity in the sizing phase. The DPD parameters (presented in Ref. 24) suggest that the compatibility between RA and SA is better than that between DDS and SA. However, much longer RA chains are unfavorable to molecule motions.

The component content at the carbon fiber surface is plotted as a function of the diffusion and/or crosslink time in Figure 3, to give a quantitative view, in which 0–40 min is solely for diffusion and 40–160 min is for simultaneous diffusion/crosslink process. Note that the amines are all generated by DDS, which are plotted in one line in Figure 3. It reveals that at the carbon fiber surface the RA and DDS concentrations both increase considerably during the first diffusion stage. However, negligible change can be found for all the components during the second diffusion/crosslink stage. This indicates that mutual diffusions are mainly achieved before the initiation of chemical reactions.

One stage of diffusion/crosslink simulation was also conducted at 180°C. Figure 4(a) shows that scant DDS can diffuse into the sizing phase (0–24 nm), according to the distribution of the reacted amines, and in Figure 4(b) the SA exists mainly in the original scope of 0–24 nm. For the two-stage simulation, the distributions of DDS and SA, generated by the first stage, are quite similar to the corresponding distributions generated by the second stage. This again demonstrates that after initiation of the crosslink reactions mutual diffusions will be extremely inhibited. Because there is minimal reactive agent in the sizing layer, we can infer that, in order to achieve sufficient crosslink in vicinity of the fiber surface, a period of only diffusion process, with negligible chemical reaction, is necessarily important. Fortunately, two-stage temperature schemes are always adopted

in manufacture engineering to improve the quality of composite parts, particularly for the high-temperature curing epoxy matrix.³³ Therefore, this two-stage temperature scheme will enhance the interphase property of the CF/epoxy composites.

Considering that the component diffusions are negligible during the diffusion/crosslink process, namely the crosslink reaction will inevitably restrain the diffusion behavior, therefore, in the following sections of Effect of Diffusion Temperature on the Interphase Region and Effect of Sizing Layer on the Interphase Region, the component distributions are all simulated by only diffusion stage to analyze effects of temperature and sizing layer on the composition and width of the transition interphase region.

Effect of Diffusion Temperature on the Interphase Region

To give a quantitative view of the temperature effect, a “relative diffusion equilibrium” state is defined as 1% DDS molecules occur in the 3 nm vicinity of the fiber surface in the simulations. Note that no hardener agent originally exists in the sizing layer in T3-Siz-RA system. The results show that it needs 279, 128, and 65 min for DDS to reach the “relative diffusion

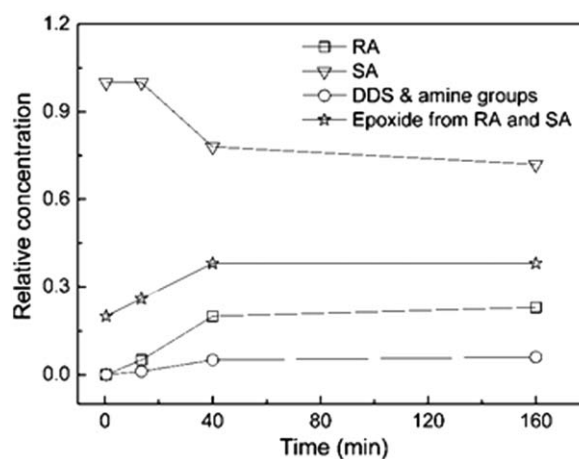


Figure 3. Plots of the component contents (at carbon fiber surface) versus time, in which the beginning 0–40 min is solely for diffusion, and the following 40–160 min is for diffusion/crosslink at 180°C.

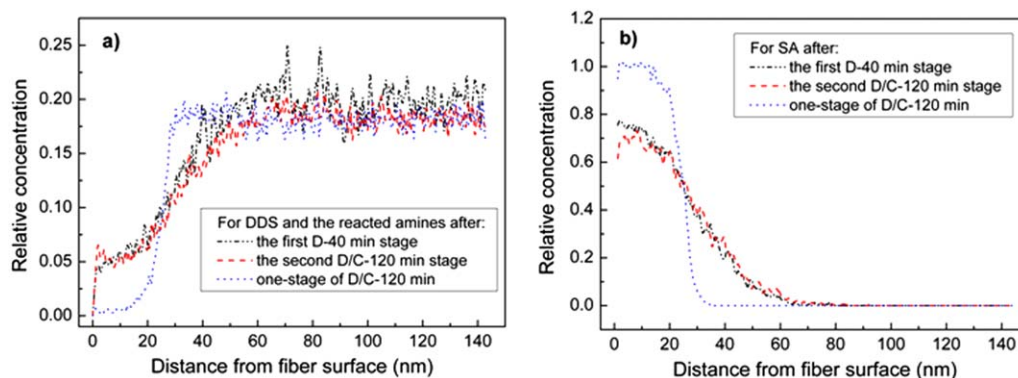


Figure 4. The concentration profiles of: (a) DDS and the corresponding reacted amines, and (b) SA, after different simulation schemes at 180°C, wherein “D” denotes only diffusion and “D/C” denotes simultaneous diffusion/crosslink. [Color figure can be viewed in the online issue, which is available at wileyonlinelibrary.com.]

equilibrium” state at 110, 150, and 180°C, respectively. The 110°C case suggests that the diffusion generating distributions of RA and DDS are quite similar between 80 and 120 min moment as shown in Figure 5(a). After diffusion for 279 min, a certain amount of RA and DDS molecules occur at the fiber surface, reaching the “relative diffusion equilibrium.” For the diffusion at 150°C [see Figure 5(b)], RA and DDS molecules can diffuse throughout the sizing layer and occur at the fiber surface after only 40 min, which indicates much faster diffusing dynamic at 150°C than that at 110°C. Thereafter, the content of RA increases considerably at the fiber surface and the DDS content increases slightly. After 128 min, 1% DDS molecules occur in 0–3 nm scope, reaching the “relative diffusion equilibrium.” From the distributions of RA and DDS in Figure 5(b), width of the gradient transition region is estimated to be 70 nm at the “relative diffusion equilibrium.” This is consistent with the width at “relative diffusion equilibrium” of 180°C case [i.e., 65 min in Figure 2(a)]. However, for the diffusion at 110°C, the width is larger than 100 nm at “relative diffusion equilibrium” in Figure 5(a).

The epoxide content (from RA and SA) at the carbon fiber surface is plotted as function of diffusion time in Figure 6(a). For the 150 and 180°C cases, the epoxide contents present approximately linear increasing tendencies with the diffusion in

progress. Higher the temperature, the faster is the diffusion velocity. The RA content remains the original 0.20 until after 120 min in the 110°C case. According to gradient distributions of the epoxide groups (not shown), widths of the transition region were evaluated. Figure 6(b) shows that the gradient widths for 110°C/80 min and 110°C/120 min both are <35 nm due to minimal inter-diffusion, whereas the width for 110°C/279 min is 105 nm. The width of 150°C/40 min diffusion is about 45 nm. Moreover, the 150°C/60 min and 180°C/40 min cases similarly present 70-nm wide of the transition region, which are consistent with the experimental data of the carbon fiber/epoxy composite (not shown). Note that 180°C is standard curing temperature of RA and DDS resin system, at which chemical reactions will be actually initiated. However, the reactions are simulated switched off during the diffusing stage in this article. Therefore, in order to obtain appropriately strong interphase of carbon fiber/epoxy, 150°C is more preferable rather than 180°C in practice.

Effect of Sizing Layer on the Interphase Region

It should be noticed that, unless otherwise specified, all the above simulation results are conducted by the T3-Siz-RA simulation system. To elucidate effect of sizing layer on the interphase formation, two other simulation systems (T3-Sizcur-RA and C3-Siz-RA) were also studied. The detail constructions are

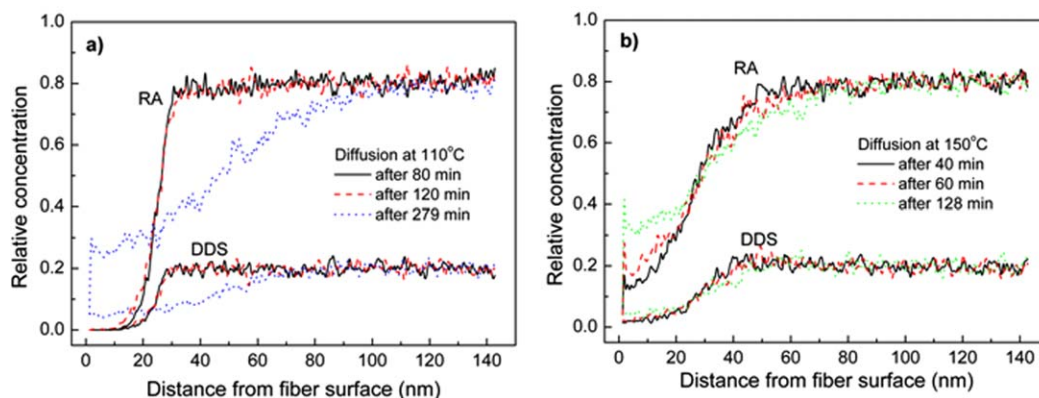


Figure 5. The distribution evolution of RA and DDS during the diffusion stage at: (a) 110°C and (b) 150°C, respectively. [Color figure can be viewed in the online issue, which is available at wileyonlinelibrary.com.]

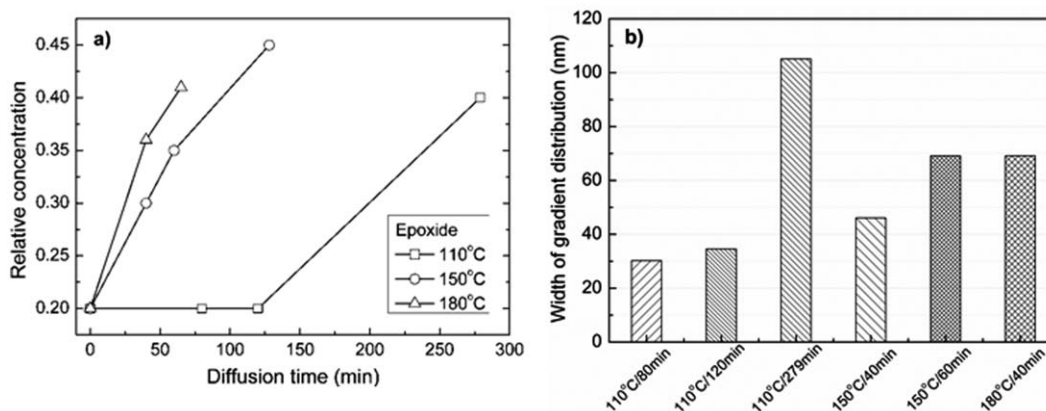


Figure 6. (a) Plot of epoxide contents at carbon fiber surface as a function of diffusion time at constant temperatures; (b) widths of the gradient distribution region of the epoxide generated by different diffusion schemes.

listed in Table I. In T3-Sizcur-RA, the sizing layer was consisted of hardener agent and long-chain epoxy. In C3-Siz-RA, the sizing layer was 36-nm thick, while in T3-Siz-RA and T3-Sizcur-RA, the sizing was 24 nm, namely, the fiber sizing amount is larger for C3-Siz-RA system. Comparison between T3-Siz-RA and T3-Sizcur-RA is plotted in Figure 7(a,b). From the distribution of RA in Figure 7(a), negligible difference can be observed for the two simulation systems, suggesting that existence of the hardener in the sizing layer has no significant influence on the

diffusion behavior of RA. However, in Figure 7(b), the distributions of DDS are considerably different between T3-Siz-RA and T3-Sizcur-RA. In 0–20 nm scope, the DDS content in T3-Sizcur-RA is higher than in T3-Siz-RA, particularly at early stage when the diffusion is not evident. With the progress of mutual diffusion, difference between the two systems decreases for the DDS content. Moreover, comparison between T3-Siz-RA and C3-Siz-RA is plotted in Figure 7(c,d). It shows that the sizing amount can significantly affect the component distributions.

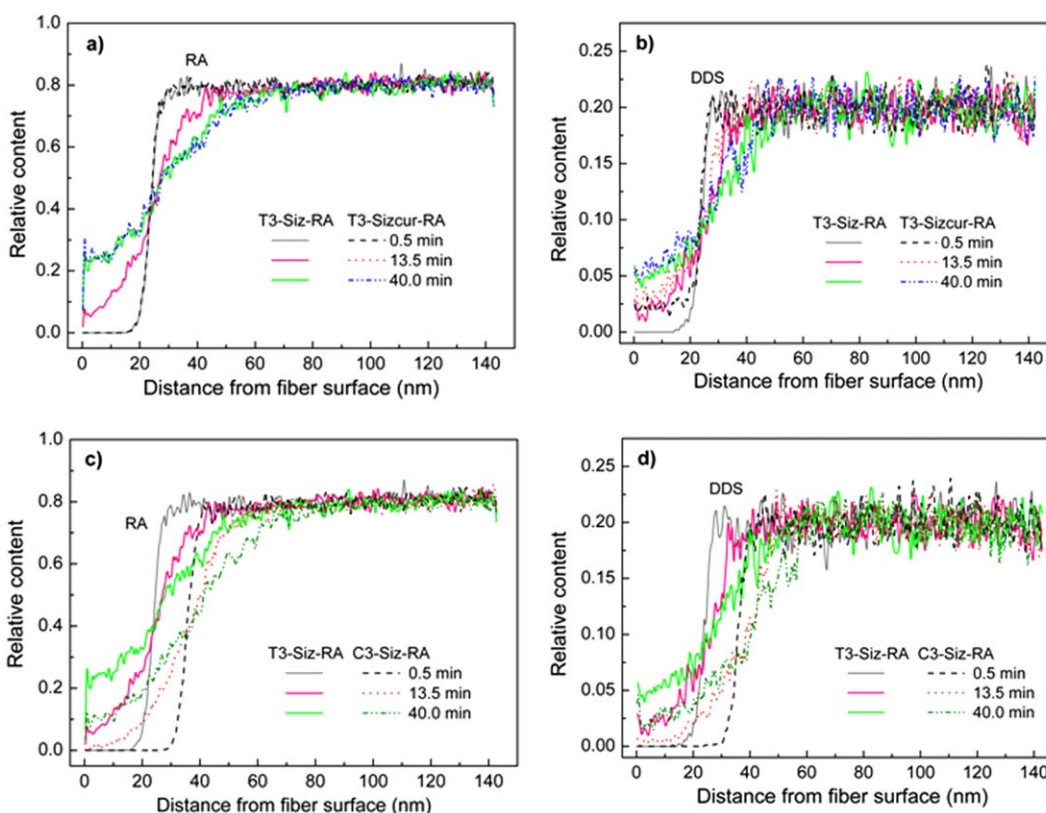


Figure 7. The distribution evolutions of RA and DDS during the diffusion at 180°C. The comparison between T3-Siz-RA and T3-Sizcur-RA is plotted in (a) and (b); and the comparison between T3-Siz-RA and C3-Siz-RA is shown in (c) and (d). [Color figure can be viewed in the online issue, which is available at wileyonlinelibrary.com.]

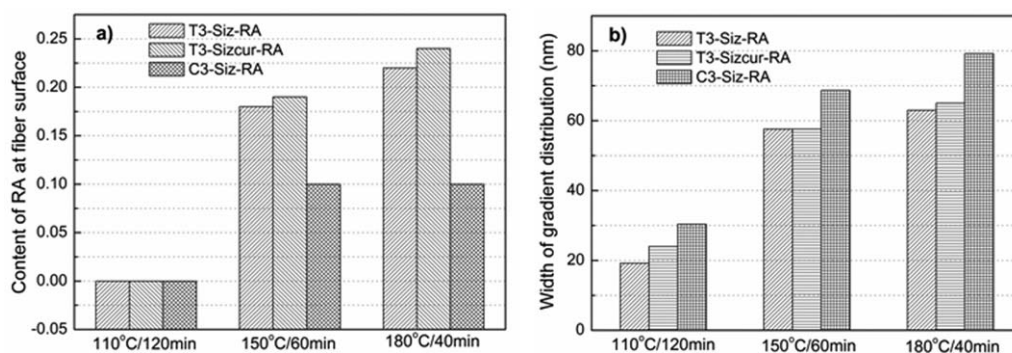


Figure 8. The distributions of RA in T3-Siz-RA, T3-Sizcur-RA, and C3-Siz-RA systems, illustrated by: (a) the RA content at carbon fiber surface; and (b) widths of the gradient distribution of RA.

In C3-Siz-RA, the RA and DDS contents are much lower within the fiber surface vicinity and widths of the transition regions are much wider than those in the T3-Siz-RA system. Because there are minimal hardener agent in carbon fiber sizing, thereby, thickness of the sizing layer is crucial in determining the reactive component concentrations, particularly in close vicinity of the fiber surface, which will inevitably impact crosslink density of the resulted interphase region.

Figure 8 presents a quantitative view of the transition distributions of RA in the three systems, due to various diffusing conditions. For the 110°C/120 min case, Figure 8 indicates minimal interdiffusion in all the systems. For the 150°C/60 min case, the RA content increases to 0.10 in C3-Siz-RA, while it is more than 0.18 in T3-Siz-RA and T3-Sizcur-RA. Meanwhile, the gradient distribution width is 69 nm for C3-Siz-RA, however, it is 58 nm in both T3-Siz-RA and T3-Sizcur-RA. For the 180°C/40 min case, comparing the three systems, similar distribution trends of RA are revealed. Therefore, we can conclude that thicker sizing layer will lead to less crosslink and wider transition region around the fiber surface, and a small amount of hardener in the sizing layer will slightly improve the crosslink density within the transition region but will not considerably change the transition width. These results can supply molecular details for optimizing in the interphase region, so as to improve load transfer efficiency in the carbon fiber/epoxy composites.

CONCLUSIONS

The mutual diffusion and crosslink behavior of epoxy, hardener and sizing agents are investigated to simulate the formation process of interphase region in carbon fiber/epoxy composites by using a multiscale simulation method. It demonstrates that sufficient mutual diffusion will result in gradient distribution of components along the fiber radial direction, crossing the interphase region. Initiation of the crosslink reactions can extremely restrain the mutual diffusion behavior of the components. Because there is minimal reactive agent in the carbon fiber sizing, two-stage temperature scheme, i.e., a period of only diffusion process, is necessary to achieve sufficient crosslink within the transition interphase region around the fiber surface. Molecular diffusion velocities can be accelerated by high temperature. The 150 and 180°C diffusion tend to result in higher concentration of crosslink points within the interphase region. In con-

trast, at 110°C the diffusions are relatively slow and insufficient. Considering practical manufacture temperature of the composite parts, 150°C is preferable to obtain appropriately strong interphase of the carbon fiber/epoxy composite. Moreover, the sizing layer has profound effect on the composition and width of the transition interphase region, particularly on the amount of reactive groups at the fiber surface. Thicker sizing layer of the carbon fiber always result in less crosslink and wider transition region, while a certain amount of hardener agent in the fiber sizing can generate a transition region with higher crosslink density and appropriate width.

ACKNOWLEDGMENTS

Financial supports from the National Natural Science Fund Program (51273007) and the Program for New Century Excellent Talents in University (NCET) are gratefully acknowledged.

REFERENCES

- Jones, F. R. *Key Eng. Mater.* **1996**, *116*, 41.
- Kim, J. K.; Mai, Y. W. *Engineered Interfaces in Fiber Reinforced Composites*; Elsevier, Netherlands, **1998**; Chapter 4, p 93.
- Gao, S. L.; Mader, E.; Plonka, R. *Adv. Mater. Eng.* **2004**, *6*, 147.
- Gohil, P. P.; Shaikh, A. A. *J. Reinf. Plast. Comp.* **2010**, *29*, 685.
- Maligno, A. R.; Warrior, N. A.; Long, A. C. *Comp. Sci. Tech.* **2010**, *70*, 36.
- Fisher, F. T.; Brinson, L. C. *Comp. Sci. Tech.* **2001**, *61*, 731.
- Romanowicz, M. *Compos A.* **2010**, *41*, 1829.
- Dai, Z. S.; Zhang, B. Y.; Shi, F. H.; Li, M.; Zhang, Z. G.; Gu, Y. Z. *J. Appl. Polym. Sci.* **2012**, *124*, 2127.
- Drzal, L. T.; Rich, M. J.; Koenig, M. F.; Lloyd, P. F. *J. Adhes.* **1983**, *16*, 133.
- Dai, Z. S.; Zhang, B. Y.; Shi, F. H.; Li, M.; Zhang, Z. G.; Gu, Y. Z. *J. Appl. Polym. Sci.*, **2012**, *124*, 2127.
- Zhang, R. L.; Huang, Y. D.; Liu, L.; Tang, Y. R.; Su, D.; Xu, L. W. *Appl. Surf. Sci.* **2011**, *257*, 3519.
- Li, M.; Yuang, C.; Wang, S. K.; Gu, Y. Z.; Potter, K.; Zhang, Z. G. *J. Appl. Polym. Sci.* **2012**, *263*, 326.

13. Komarov, P. V.; Chiu, Y. T.; Chen, S. M.; Khalatur, P. G.; Reineker, P. *Macromolecules* **2007**, *40*, 8104.
14. Duering, E. R.; Kremer, K.; Grest, G. S. *Phys. Rev. Lett.* **1991**, *67*, 3531.
15. Kenkhare, N. R.; Smith, S. W.; Hall, C. K.; Khan, S. A. *Macromolecules*. **1998**, *31*, 5861.
16. Lu, Z. Y.; Hentschke, R. *Phys. Rev. E* **2001**, *63*, 051801, 1–8.
17. Lu, Z. Y.; Hentschke, R. S. *Phys. Rev. E* **2002**, *66*, 041803, 1–8.
18. Aydt, E. M.; Hentschke, R. *J. Chem. Phys.* **2005**, *123*, 054902, 1–8.
19. Liu, H.; Li, M.; Lu, Z. Y.; Zhang, Z. G.; Sun, C. C.; Cui, T. *Macromolecules* **2011**, *44*, 8650.
20. Liu, H.; Li, M.; Lu, Z. Y.; Zhang, Z. G.; Sun, C. C. *Macromolecules* **2009**, *42*, 2863.
21. Yarovsky, I.; Evans, E. *Polymer* **2002**, *43*, 963.
22. Wu, C. F.; Xu, W. J. *Polymer* **2006**, *47*, 6004.
23. Hörstermann, H.; Hentschke, R.; Amkreutz, M.; Hoffmann, M.; Wirts-Rütters, M. *J. Phys. Chem. B* **2010**, *114*, 17013.
24. Li, M.; Gu, Y. Z.; Liu, H.; Li, Y. X.; Wang, S. K.; Wu, Q.; Zhang, Z. G. *Comp. Sci. Tech.* **2013**, *86*, 117.
25. Toth, R.; Voorn, D. J.; Handgraaf, J. W.; Fraaije, J. G.; Fermeglia, M.; Pricl, S.; Posocco, P. *Macromolecules* **2009**, *42*, 8260.
26. Groot, R. D.; Warren, P. B. *J. Chem. Phys.* **1997**, *107*, 4423.
27. Lowe, C. P. *Europhys. Lett.* **1999**, *47*, 145.
28. Chen, L. J.; Qian, H. J.; Lu, Z. Y.; Li, Z. S.; Sun, C. C. *J. Phys. Chem. B* **2006**, *110*, 24093.
29. Chen, L. J.; Lu, Z. Y.; Qian, H. J.; Li, Z. S.; Sun, C. C. *J. Chem. Phys.* **2005**, *122*, 104907.
30. Zhao, Y.; You, L. Y.; Lu, Z. Y.; Sun, C. C. *Polymer* **2009**, *50*, 5333.
31. Fermeglia, M.; Cosoli, P.; Ferrone, M.; Piccarolo, S.; Mensitieri, G.; Pricl, S. *Polymer* **2006**, *47*, 5979.
32. Liu, H.; Qian, H. J.; Zhao, Y.; Lu, Z. Y. *J. Chem. Phys.* **2007**, *127*, 144903.
33. Gu, Y. Z.; Li, M.; Zhang, Z. G.; Sun, Z. J. *J. Comp. Mater.* **2006**, *40*, 2257.